

Effects of sulfur isotopic composition on the band gap of PbS

H. J. Lian, A. Yang, and M. L. W. Thewalt*

Department of Physics, Simon Fraser University, Burnaby, BC, V5A 1S6, Canada

R. Lauck and M. Cardona

Max Planck Institut für Festkörperforschung, Stuttgart, Germany

(Received 27 March 2006; published 12 June 2006)

Low temperature photoluminescence spectra of synthetic PbS crystals having the natural isotopic abundance (95% ^{32}S) are compared with crystals grown using 99% ^{34}S . An anomalous *decrease* in the band gap energy of $6.5 \pm 2 \text{ cm}^{-1}$ with increasing S mass was observed. The unusual sign of this isotope shift can be related to the temperature dependence of the band gap energy, which opposite to the behavior seen for most common semiconductors, *increases* strongly between 2 K and 320 K. This temperature dependence was measured with improved accuracy using absorption spectroscopy, and a fit to this data suggests that there should be virtually no net renormalization of the band gap energy due to zero point motion at low temperatures. This must result from a cancellation of the contributions from S and Pb, but the predicted “normal” isotope shift of the band gap energy with Pb mass is too small to be measured.

DOI: [10.1103/PhysRevB.73.233202](https://doi.org/10.1103/PhysRevB.73.233202)

PACS number(s): 78.30.Hv, 78.55.Hx

I. INTRODUCTION

Thanks to its availability in nearly perfect single crystal form as the mineral galena, PbS is one of the earliest semiconductors to have been used and investigated.^{1,2} Thanks to their direct electronic gaps which occur at infrared frequencies, the lead chalcogenides have found applications in infrared detector and laser technology^{3,4} and as materials for research into the properties and applications of quantum dots.⁵ Their thermodynamic,^{6,7} electrical, optical,⁸ photoelectric,⁹ and vibrational^{10–13} properties have been thoroughly investigated.¹⁴ PbS crystallizes in the rock salt structure (space group $Fm\bar{3}m$) and has four equivalent direct band gaps at the L points of the Brillouin zone. Due to the small electron and hole effective masses and the very large dielectric constant,¹⁴ Coulomb bound states such as shallow neutral donors and acceptors, and excitons, are not observed even at the lowest temperatures.

One of the interesting features of PbS and the other lead chalcogenides is the strong *increase* of the band gap energy with increasing temperature,^{14,15} opposite to what is observed for all of the more common semiconductors. This behavior led us to investigate the dependence of the PbS band gap energy in the low temperature limit on isotopic composition, since the same two processes which determine the temperature dependence of the band gap energy—the renormalization of the band gap energy by the electron-phonon interaction and the temperature dependence of the lattice constant (together with the volume dependence of the band gap energy)—also determine the dependence of the band gap energy on the isotopic masses in the low temperature limit.¹⁶ The influence of the isotopic composition on the physical properties of semiconductors has received considerable attention over the past two decades, as outlined in a recent review,¹⁶ in part due to the availability of macroscopic quantities of highly enriched stable isotopes of most elements at prices which allow for the synthesis of small bulk crystals or epitaxial samples.

We have studied the dependence of the PbS band gap energy on S isotopic mass by comparing the low temperature

photoluminescence spectra of synthetic PbS crystals produced with S of natural isotopic composition (95% ^{32}S , 0.75% ^{33}S , 4.2% ^{34}S , 0.02% ^{36}S) and highly enriched (99%) ^{34}S . The band gap energy was found to *decrease* by $6.5 \pm 2 \text{ cm}^{-1}$ for the heavier S isotope, opposite to the usual *increase* in the gap with increasing mass. The temperature dependence of the band gap energy from 2 to 320 K was determined with improved accuracy using transmission spectroscopy on thin samples of natural PbS, since the existing data^{14,15} did not match well between the lowtemperature and higher temperature regions, and was inadequate for a determination of the net renormalization of the band gap energy due to zero point motion of the constituent atoms in the limit of low temperature. The new temperature dependence data was accurately fit with a three oscillator model, and indicated essentially zero net renormalization of the gap at low temperatures. Since a significant isotope shift was observed when changing the S mass, this suggested a cancellation between the contributions of S and Pb to the net band gap renormalization at $T=0$, but the expected “normal” isotope shift when varying the Pb mass will likely be too small to be directly observed.

II. SAMPLES

The samples used in the present study are identical to those used in a recent investigation on the effects of temperature and S isotopic mass on the Raman spectrum of PbS, and their characteristics and the method of preparation of the synthetic samples are described in detail there.¹³ All of the samples studied here were p -type, with hole concentrations of $8.9 \times 10^{17} \text{ cm}^{-3}$ for the Pb^{34}S sample, $1.7 \times 10^{18} \text{ cm}^{-3}$ for the synthetic sample grown using natural S , and $2.1 \times 10^{17} \text{ cm}^{-3}$ for the natural galena sample, as determined by the energy of the plasmons edge measured by infrared reflectance spectroscopy.¹³ The natural galena sample was obtained from Creede, CO, and is referred to as such in the earlier Raman studies.^{12,13} The Creede material was used to

determine the temperature dependence of the PbS band gap using infrared absorption spectroscopy since it had the lowest carrier concentration, and thus the greatest transparency at energies below the band gap. It was also available as large single crystals, from which the $45\ \mu\text{m}$ thick sample was obtained by mechanical polishing. The synthetic samples were smaller, with $\sim 1\ \text{mm}$ squared (100) faces having macroscopic ($\sim 0.1\ \text{mm}$) steps. These samples were used for the photoluminescence study without further preparation.

III. EXPERIMENTAL RESULTS

For the photoluminescence measurements, the PbS crystals were freely suspended in superfluid liquid helium in a dewar having sapphire windows. Excitation was provided by the multiline visible output of an Argon ion laser, at powers of 50 and 5 mW in an unfocused beam with a diameter of $\sim 3\ \text{mm}$. No change in the line shape was observed between these two excitation levels, indicating that sample heating was not significant. The luminescence was collimated by an off-axis parabolic mirror and sent into the interferometer through a CaF_2 window, with the path between the dewar window and the interferometer window purged with dry N_2 gas to eliminate interference from water vapor absorption lines. The luminescence was analyzed using a Bomem DA8 Michelson interferometer at a resolution of $0.5\ \text{cm}^{-1}$ with a CaF_2 beam splitter and a liquid nitrogen cooled InSb photovoltaic detector. A 1038 nm long pass filter was placed between the interferometer and the detector to eliminate scattered argon-ion laser light, and the scattered light from the internal interferometer alignment laser (632.8 nm). The room temperature blackbody background spectrum was collected under identical conditions but with zero excitation power, and subtracted from the photoluminescence spectra. Spectra were collected from several crystals of each of the two growth runs, and were found to be essentially identical. Interestingly, no photoluminescence could be observed from the natural galena sample from Creede CO, indicating that although this material had the lowest free carrier concentration, it must also have contained recombination centers which competed with radiative recombination.

In Fig. 1 we compare typical liquid He temperature photoluminescence spectra of the synthetic $\text{Pb}^{\text{nat}}\text{S}$ and Pb^{34}S samples. The spectra are seen to be quite similar in shape, with that of the Pb^{34}S sample being shifted down by $6.5\ \text{cm}^{-1}$ from that of the $\text{Pb}^{\text{nat}}\text{S}$ sample. The uncertainty of $\pm 2\ \text{cm}^{-1}$ reflects the small differences in the two line shapes, together with the small shifts observed in spectra from different samples of the same materials.

As can be seen in the photoluminescence spectra of Fig. 1, the accurate measurement of the difference in band gap energy between $\text{Pb}^{\text{nat}}\text{S}$ and Pb^{34}S is made difficult by the rather broad optical transitions resulting from the recombination of free electrons in the conduction band with free holes in the valence band. In other semiconductors, the presence of sharp excitonic luminescence and absorption transitions permits the determination of small differences in band gap energy with remarkable precision,¹⁶ but in PbS this is not possible due to the vanishingly small binding energies of

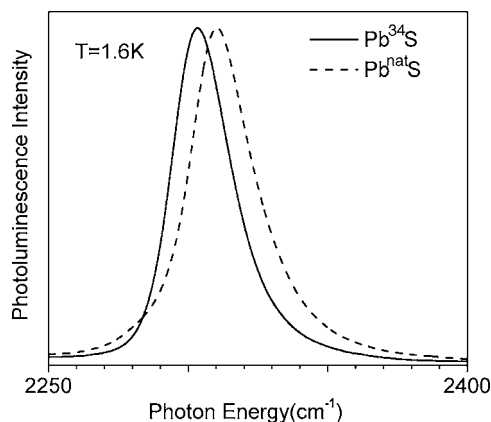


FIG. 1. Low temperature photoluminescence spectra of PbS samples grown using natural S ($\sim 95\% \text{ }^{32}\text{S}$) and highly enriched ^{34}S are compared. The measured value of the peak shift is $6.5 \pm 2\ \text{cm}^{-1}$.

excitons and shallow impurity states resulting from the small carrier effective masses and the large dielectric constant.¹⁴ The spectra from the two materials are at least very similar in shape, as would be expected from the fact that both received the same purification, growth, and annealing treatments and are therefore expected to have similar impurity and defect content, as verified by their similar free carrier concentrations. The luminescence spectra do have asymmetrical tails towards higher energy, as would be expected from the recombination of a thermal distribution of electrons in the conduction band (at an effective temperature which may be above that of the lattice) with a similar distribution of free holes in the valence band (which may be at a different effective temperature). Unfortunately the luminescence lines do not have the sharp low energy cutoff which would be expected from this simple plasma recombination model, showing instead a weaker tail towards lower energy which likely results from the impurity or defect-induced Urbach tails¹⁷ of the band edges. The more pronounced low energy tail and broadening of the $\text{Pb}^{\text{nat}}\text{S}$ sample are consistent with its ~ 2 times higher free carrier concentration. The stated shift of $6.5 \pm 2\ \text{cm}^{-1}$ between the two spectra is consistent with both the shift between the two peaks and the shift between the zero intercepts of a linear extrapolation of their low energy edges.

The temperature dependence of the band gap energy shown in Fig. 2 was determined by measuring the absorption edge of a $45\ \mu\text{m}$ thick sample of the natural Creede galena mounted freely between two sapphire plates in He gas in a Varitemp dewar having ZnSe windows, and using the same interferometer and detector as for the photoluminescence measurement, together with a quartz-halogen white light source. The temperature of the Cu block upon which the sapphire plates enclosing the sample were mounted was regulated by a Lakeshore 805 temperature controller and a calibrated Si diode temperature sensor.

IV. DISCUSSION

The connection between the temperature dependence of the band gap energy and its dependence on the isotopic

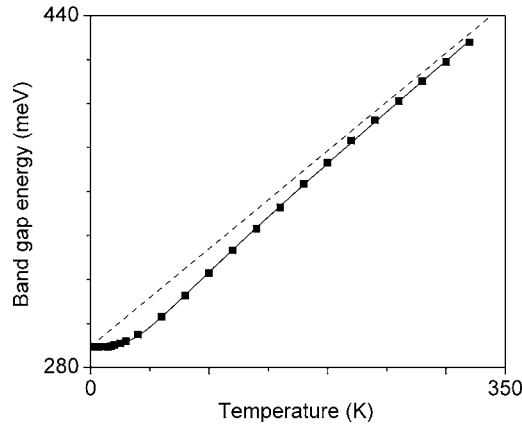


FIG. 2. The temperature dependence of the band gap of natural PbS as determined by absorption spectroscopy is plotted from 2 to 320 K. The solid line is a fit to the data using a three oscillator model as described in the text. The dashed line, which has a slope of ~ 0.45 meV/ $^{\circ}$ K, is an extrapolation of a linear fit to the model in the high temperature limit. The near-agreement of this extrapolation and the observed $T \approx 0$ band gap energy indicates that there is essentially no net zero-point renormalization of the band gap energy at low temperature in PbS.

mass(es) has been investigated in many semiconductors, and has recently been reviewed in considerable detail.¹⁶ Both phenomena have the same two fundamental causes—the renormalization of the band gap energy by the electron-phonon interaction, and the variation of the band gap energy with changing lattice constant, together with the dependence of the lattice constant on the vibrational amplitudes of the constituent atoms. In most semiconductors the contribution of the electron-phonon effect dominates over that of the change in lattice constant, and it is often considered to be the only important term.¹⁶ While detailed information on the temperature dependence of the lattice constant is not available for PbS, the values available for $T > 35$ K,¹⁸ together with the bulk modulus of 50 GPa at room temperature¹⁹ and the room temperature pressure derivative of the band gap energy of -9.1×10^{-6} eV/bar (Ref. 20) can be used to estimate that half of the change in band gap energy with the temperature seen in Fig. 2 results from the change in lattice constant. In the absence of more detailed information, we will hereafter consider only the net effect of both the electron-phonon interaction and the changes in lattice constant, since both of these terms have a similar dependence on the phonon population factors, the vibrational amplitudes, and the atomic masses.

The temperature dependence of the band gap energy shown in Fig. 2 can be used to determine the net renormalization of the band gap energy due to zero point motion in the limit of low temperature, or in other words, the energy difference between the observed low temperature band gap energy and the (not directly observable) “bare” band gap energy which would be obtained in the limit of zero amplitude atomic motion (or, in other words, the limit of infinite atomic masses). If the temperature dependence data extends to the high temperature limit, where it becomes accurately linear, then the net renormalization can be determined as the

difference between the observed low temperature band gap energy and the value obtained by extrapolating to $T=0$ the linear high temperature behavior. However, the data in Fig. 2 does not extend to the high temperature limit, as a small negative curvature is observable even at the highest temperatures. In such cases the net $T=0$ renormalization can still be obtained from an accurate fit to the available data using a multioscillator model.¹⁶

To fit the data of Fig. 2 we have used a model consisting of three Bose-Einstein oscillators which can be represented by:

$$E(T) = E_0 + E_1 \left(2 \times \frac{1}{e^{f_1/kT} - 1} + 1 \right) + E_2 \left(2 \times \frac{1}{e^{f_2/kT} - 1} + 1 \right) + E_3 \left(2 \times \frac{1}{e^{f_3/kT} - 1} + 1 \right) \quad (1)$$

where E_0 is the “bare” band gap energy, $E_1 + E_2 + E_3$ is the net renormalization energy at $T=0$, and f_1 , f_2 , and f_3 are the energies of the three oscillators, for which we have used, respectively, 50, 93, and 225 cm^{-1} . These oscillator frequencies were obtained from the phonon density of states for PbS (Refs. 10 and 11), and small changes in their values do not affect the quality of the fit, or the physical results obtained from the fit. The parameters obtained from the best fit (shown as the solid line in Fig. 2) are $E_0 = 290.6$ meV, $E_1 = 5.4$ meV, $E_2 = 38.3$ meV, and $E_3 = -44.8$ meV. Thus the net renormalization of the band gap energy at $T=0$ is found to be -1.1 meV, which is equal to zero within the expected accuracy of the procedure.

On the other hand, a clear isotope effect of the S mass on the band gap energy was observed, as seen in Fig. 1. From the shift of -3.5 ± 1 $\text{cm}^{-1}/\text{amu}$ (-0.43 ± 0.12 meV/amu), the net $T=0$ band gap renormalization *due to S* can be calculated, since for a given constituent the renormalization from both the electron-phonon effect and the lattice constant effect vary as the inverse square root of the mass of the atom involved. Thus the total net band gap renormalization at $T=0$ due to the zero point motion of the S atoms is found to be $+234 \pm 70$ cm^{-1} ($+29 \pm 9$ meV). In order to account for the negligible total renormalization of the band gap energy obtained from the temperature dependence data, we must therefore assume that the contribution of the zero point motion of the Pb cancels that of the S , or in other words that the net $T=0$ band gap renormalization due to the zero point motion of Pb is approximately -234 cm^{-1} (-29 meV). Using again the fact that the renormalization for a given constituent goes as the inverse square root of the mass, we can predict a “normal” isotope shift for Pb in PbS of approximately $+0.55$ $\text{cm}^{-1}/\text{amu}$ ($+0.068$ meV/amu). Given the range of stable isotopes of Pb which are available, and the lack of sharp excitonic transitions in PbS, it is unlikely that this small isotope shift expected for Pb can be directly verified.

These results for PbS are similar in many ways to earlier results obtained for CuCl ²¹ and the other cuprous halides.²² The cuprous halides also have anomalous positive temperature coefficient of the band gap energy, although to a lesser extent than PbS (for CuI the coefficient tends to zero in the limit of high temperature). They also show the “anomalous”

decrease in band gap energy with increasing Cu mass which was observed here for S in PbS. A fit to the temperature dependence of the cuprous halide band gap energies also suggested a cancellation between the contributions of the zero point motions of Cu and the halogen species on the renormalization of the band gap in the limit of low temperature. For CuI the cancellation was essentially complete, similar to what we report here for PbS. However, unlike the present case, for CuCl and CuBr the isotope shifts of the band gap energy in the low temperature limit could be observed directly for both the Cu and the halogen constituents, and the net band gap renormalization remaining after the partial cancellation of their contributions agreed well with net renormalization predicted from the temperature dependence of the band gap energy.^{21,22}

Information about the separate contributions of Pb and S to the zero point renormalization of the gap can also be obtained from the fitted energies E_1 , E_2 , E_3 of Eq. (1) if one knows the average displacements of the Pb and S atoms (eigenvectors) which correspond to the average frequencies f_1 , f_2 , and f_3 . The highest frequency f_3 corresponds to LO phonons which involve predominantly the vibrations of S atoms. Since the E_3 obtained from the fit in Fig. 2 is negative, there must be another band of sulphur-related vibrations with a positive value of E . The large LO-TO splittings found in the lead chalcogenides^{10,11} suggests that the average frequency f_2 corresponds not only to LA vibrations involving lead but also to TO vibrations of sulfur. A large positive

contribution of the f_2 vibrations to E_2 may overcompensate the negative contribution of E_3 and thus account for the sign of the mass dependence reported in Fig. 1.

V. CONCLUSIONS

We have reported the observation of an isotope shift of the band gap of a lead chalcogenide by comparing the photoluminescence spectra of PbS samples synthesized using either natural S ($\sim 95\%$ ^{32}S) or highly enriched ^{34}S . The band gap energy was found to decrease with increasing S mass, opposite to what is normally observed in other semiconductors. The temperature dependence of the band gap energy between 2 and 320 K was measured with improved accuracy, and a three oscillator fit to this data was used to determine that there is essentially no renormalization of the band gap energy due to zero point motion at $T=0$. This result suggests that the contributions of Pb and S zero-point motion must therefore cancel. The predicted small positive isotope shift of the band gap energy with increasing Pb mass is likely to remain too small to be directly measured.

ACKNOWLEDGMENTS

A.Y. gratefully acknowledges the support of NSERC while M.L.W.T. gratefully acknowledges the support of the Canada Council (Killam).

*Corresponding author. Electronic address: mthewalt@sfu.ca

¹Yu. I. Ravich, B. A. Efimov, and I. Smirnov, *Lead Chalcogenides* (Plenum Press, New York, 1970).

²R. Dalven, *Infrared Phys.* **9**, 141 (1969).

³H. Preier, *Appl. Phys.* **20**, 189 (1979).

⁴J. Xu, A. Lambrecht, and M. Tacke, *Electron. Lett.* **30**, 571 (1994).

⁵F. W. Wise, *Acc. Chem. Res.* **33**, 773 (2000).

⁶C. Wagner, *J. Chem. Phys.* **38**, 62 (1950).

⁷G. Simkovich and J. B. Wagner, Jr., *J. Chem. Phys.* **38**, 1368 (1963).

⁸J. R. Dixon and H. R. Riedl, *Phys. Rev.* **140**, A1283 (1965).

⁹T. Grandke and M. Cardona, *Surf. Sci.* **92**, 385 (1980).

¹⁰M. M. Elcombe, *Proc. R. Soc. London, Ser. A* **300**, 210 (1967).

¹¹K. S. Upadhyaya, M. Yadav, and G. K. Upadhyaya, *Phys. Status Solidi B* **229**, 1129 (2002).

¹²G. D. Smith, S. Firth, R. J. H. Clark, and M. Cardona, *J. Appl. Phys.* **92**, 4375 (2002).

¹³R. Sherwin, R. J. H. Clark, R. Lauck, and M. Cardona, *Solid State Commun.* **134**, 565 (2005).

¹⁴*Landolt-Börnstein, Numerical Data and Functional Relationships*

in Science and Technology, edited by O. Madelung and G. Nimtz (Springer, Berlin, 1983) Vol. 17f.

¹⁵G. Nimtz and B. Slicht, *Springer Tracts in Modern Physics*, (Springer, Berlin, 1983), Vol. 98.

¹⁶M. Cardona and M. L. W. Thewalt, *Rev. Mod. Phys.* **77**, 1173 (2005).

¹⁷F. Urbach, *Phys. Rev.* **92**, 1324 (1953).

¹⁸S. I. Novikova and N. K. Abrikosov, *Sov. Phys. Solid State* **5**, 1397 (1964).

¹⁹G. I. Peresada, E. G. Ponyatovskii, and Z. D. Sokolovskaya, *Phys. Status Solidi A* **35**, K177 (1976).

²⁰V. Prakash, Technical Report No. HP-13 from the Division of Engineering and Applied Physics, Harvard University (1967) (unpublished); W. Paul and R. V. Jones, *Proc. Phys. Soc. London, Sect. B* **66**, 194 (1954).

²¹A. Göbel, T. Ruf, M. Cardona, C. T. Lin, J. Wrzesinski, M. Steube, K. Reimann, J.-C. Merle, and M. Joucla, *Phys. Rev. B* **57**, 15183 (1998).

²²J. Serrano, Ch. Schweitzer, C. T. Lin, K. Riemann, M. Cardona, and D. Fröhlich, *Phys. Rev. B* **65**, 125110 (2002).